Constructing Single- and Multiple-Helical Microcoils and Characterizing Their Performance as Components of Microinductors and Microelectromagnets

John A. Rogers, Rebecca J. Jackman, and George M. Whitesides

Abstract—**This paper describes a means for producing single- and multiple-helical microcoils by using microcontact printing to print lines on cylinders. This method was used to fabricate coils made of wires with widths and spaces between 150–25 μm wrapped around cylinders with diameters between 100–400 μm. Results show that microelectromagnets using these microcoils produce magnetic flux densities in excess of 0.4 T and can be switched on and off on a submillisecond time scale. [224]**

Index Terms—**Coils, electromagnets, fabrication, ferromagnetic materials/devices, inductors, microelectromechanical devices.**

I. Introduction

ELECTRICALLY conducting microcoils are useful in a wide variety of applications. Examples include excitation and detection coils for micro nuclear magnetic resonance (NMR) spectroscopy [1]–[4], read/write heads for magnetic data storage [5], [6], sensors for measuring magnetic fields [7]–[10] and for detecting flaws in materials [11]–[13], micropositioners [14] and microactuators [15]–[17], and microinductors [18]–[21] and transformers [22]–[25]. Since microcoils for many of these applications incorporate wires with diameters less than 100 μm, construction of these coils is not straightforward. In nearly all cases, the coils are formed either by winding a wire around a support using a micromanipulator or by using photolithography to pattern spirals on a planar substrate. The need to use wires and supports that can be manipulated limits the former, and the latter requires the use of two-dimensional (2-D) coils (i.e., spirals). In spite of the attractiveness of three-dimensional (3-D) helical microcoils for many of the applications listed above [10], [26], limitations associated with currently available means for fabrication have, with few exceptions [10], frustrated their fabrication.

In this paper, we describe a simple method for generating 3-D helical microcoils that is based on microcontact printing (μCP) [27]–[31]. We use this method to fabricate microcoils with wires between 150–25-μm wide separated by between 150–25 μm, on cylinders with diameters between 100–400 μm. We show how these microcoils can be used in conjunction with capillaries and fine ferromagnetic wire to form microelectromagnets that can produce magnetic flux densities in the range of several tenths of a Tesla and can be switched on and off on a submillisecond time scale.

Manuscript received August 21, 1996; revised January 9, 1997. Subject Editor, S. D. Senturia. This work was supported in part by the National Science Foundation (PHY-9312572), the William F. Milton Fund of the Harvard Medical School, MRSEC Shared Facilities supported by the NSF under Award DMR-9400396, the Harvard University Society of Fellows, and an NSERC scholarship.

J. A. Rogers is with Bell Laboratories, Lucent Technologies, Murray Hill, NJ 07974 USA.

R. J. Jackman and G. M. Whitesides are with the Department of Chemistry and Chemical Biology, Harvard University, Cambridge, MA 02138 USA.

Publisher Item Identifier S 1057-7157(97)06958-8.

II. Experimental

In this Section, we describe the use of microcontact printing to form microcoils. We begin by describing microcontact printing and showing how printing lines on the surface of a cylindrical substrate can form coils. We then present a method for electroplating metal onto these coils to improve their electrical and mechanical characteristics. Finally, we outline a means for forming microinductors and microelectromagnets using these coils and fine ferromagnetic wire, and we describe their characterization.

A. Fabricating Conducting Microcoils, and Microinductors with Ferromagnetic Cores

Microcontact printing (μCP) is a technique for generating patterns with high-spatial resolution on planar and curved substrates [27], [30]. It uses an elastomeric stamp, formed using photolithography or other means, to deliver ink to selected locations on a substrate. The ink can be used, for example, to prevent removal of material [29], [32] or to initiate deposition of material from an electroless plating bath [33]. This paper focuses primarily on using μCP to print resists of hexadecanethiolate monolayers on cylindrical substrates coated with silver. To coat the substrates, we installed a system of stages in an electron-beam evaporator that rotated the substrates about two orthogonal axes during the evaporation (Fig. 1). With this system, we could coat uniformly all sides of cylindrical objects with diameters less than ~2 mm in a single evaporation. For larger cylinders, partial shadowing creates a gradient in thickness around the perimeter of the cylinder. In these cases, uniform coatings can be obtained by rotating the cylinders about their axis. For the work described here, we used the system illustrated in Fig. 1 to coat glass cylinders

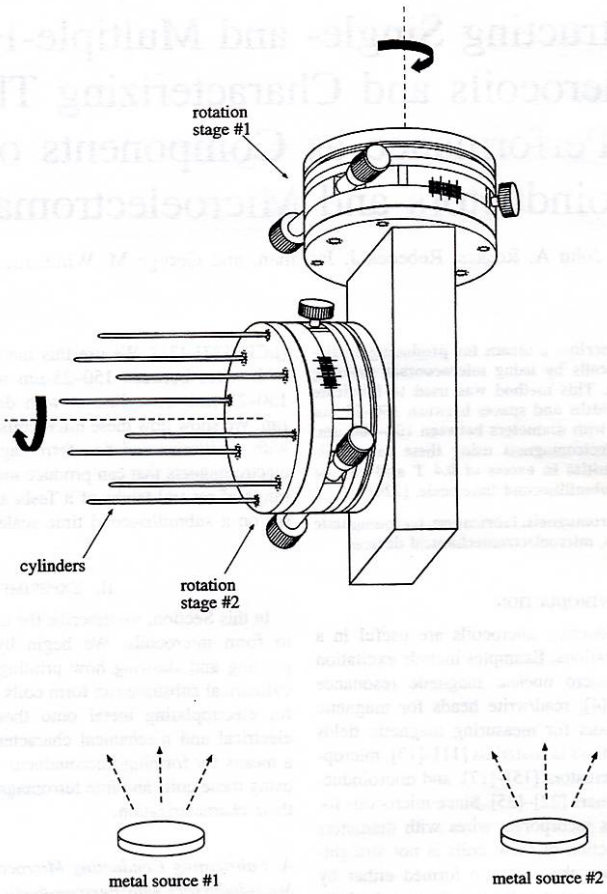

Fig. 1. Arrangement of stages that allows for rotation of samples about two orthogonal axes during evaporative deposition of materials. This system allows all sides of cylindrical objects to be coated during a single evaporation. Typical rates of rotation are on the order of one cycle per second, and times for evaporation are on the order of tens of minutes.

with diameters less than 400 μm with ~25 Å of titanium (adhesion promoter) and ~500 Å of silver.

To form microcoils, we printed lines of hexadecanethiol on the silver-coated surfaces of the glass cylinders by rolling them over the surfaces of "inked" stamps. The orientation of the lines of the stamp and the axis of the cylinder was adjusted to satisfy the relationship

$$\sin\theta = \frac{nd}{2\pi r}. \tag{1}$$

In this expression, θ is the angle between the axis of the cylinder and the lines of the stamp, d is the spacing between the lines of the stamp, r is the radius of the cylinder, and n is an integer (Fig. 2). For $n = 1$, a single helix forms from a single rotation of the cylinder over the "inked" stamp. For $n = 2, 3, \cdots$, a single rotation forms double-, triple-, and other multiple-helical structures. We set angles determined by (1) to within ~0.1° with a laser-aligned arrangement of precision translation and rotation stages [34]. We also used these stages to control the other conditions (i.e., time, pressure, and distance) of the printing.

We inserted the printed cylinders into a ferri/ferrocyanide [1-mM $K_4Fe(CN)_6$, 10-mM $K_3Fe(CN)_6$, and 0.1-M $Na_2S_2O_3$] bath for ~20 s to remove the silver not protected by the hexadecanethiol. Inserting the etched cylinders into 1% HF for 10 s removed the exposed titanium (Fig. 3).

Since many applications of microcoils require low electrical resistance or high mechanical stiffness, it is important to have the capability to fabricate microcoils with thicknesses greater than a few hundred angstroms. It is not possible to form thick coils directly using the process described in the previous paragraphs because the etch removes the hexadecanethiol resist in the time required to etch through ~1000 Å of silver.

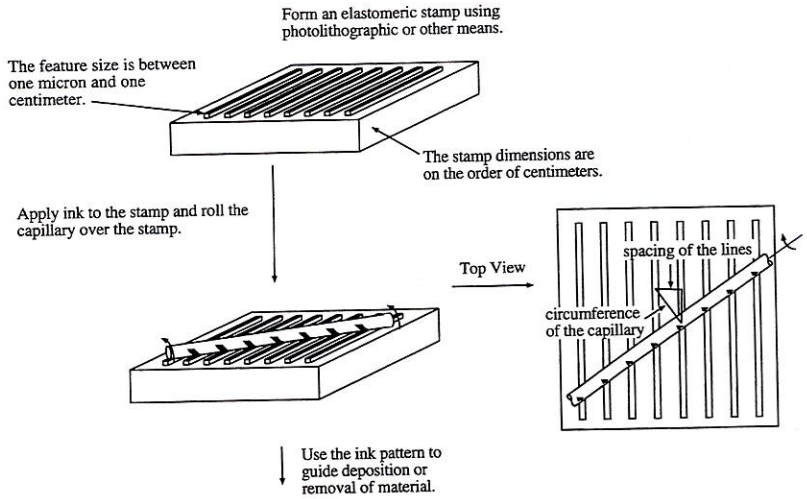

Fig. 2. Scheme for fabricating 3-D helical microcoils using microcontact printing. An inked elastomeric stamp consisting of raised lines formed using photolithographic or other means delivers ink to selected locations on a sample. When the sample consists of a cylinder and the orientation between the axis of the cylinder and the lines of the stamp is properly related to the spacing of the lines and the circumference of the cylinder, then rolling the cylinder over the stamp generates a single- or multiple-helical coil on the surface of the cylinder. The ink either initiates deposition of material or prevents its removal.

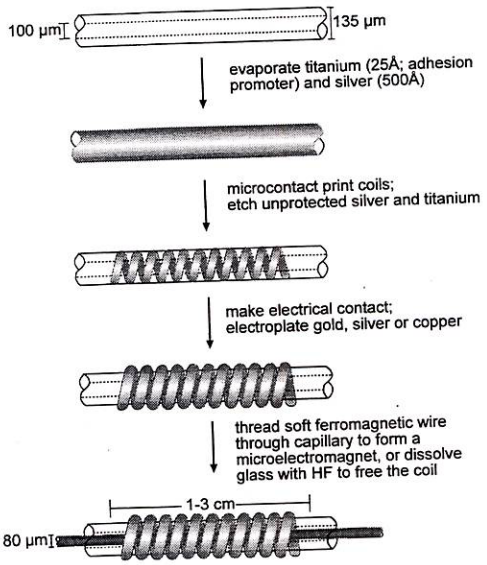

Fig. 3. Procedure for fabricating supported and free-standing microcoils, microinductors, and microelectromagnets using microcontact printing and electroplating.

The thickness of a thin coil can, however, be increased by electroplating. Using an electrical connection formed by a gold wire attached to the coil with silver epoxy, we electrodeposited copper, silver, or gold onto the coils using commercially available plating baths.

To form microinductors and microelectromagnets with ferromagnetic cores, we first removed the polyimide coating on commercially available glass capillaries (outer diameter $\sim$135 μm, inner diameter $\sim$100 μm, Polymicro Technologies, Inc., Phoenix, AZ) using a resistively heated filament. We then generated coils on these capillaries using procedures described above and electroplated gold onto the coils (Technic Orotemp 24, Technic, Providence, RI) at current densities of $\sim$4 mA/cm^2 for several minutes. Threading fine (diameter 80 $\pm$ 1 μm) wire (California Fine Wire, Grover Beach, CA) made from a soft magnetic material [80% Ni, 15% Fe, 4.4% Mo, and 0.6% other (MONIFE 479)] into the cores of the capillaries increased the inductances (magnetic flux density) of the microinductors (microelectromagnets) (Fig. 3).

B. Characterizing the Microinductors and Microelectromagnets with Ferromagnetic Cores

We made the electrical connection to the microcoils with fine gold wire and silver epoxy and measured the current as a function of applied voltage. This measurement was performed on silver coils before and after electroplating gold.

Using an inductance/capacitance/resistance (LCR) meter (Hewlett-Packard 4284 A with internal dc bias and test fixture 16 334 A SMD), we determined the inductance (L) and the resistance (R) as a function of the: 1) frequency; 2) magnitude of the current used for the test; and 3) magnitude of a constant bias current applied during the test. We modeled our structures as purely resistive elements in series with purely inductive ones and determined the resistance and inductance of various lengths of gold-plated coils with wires 150, 50, and 25 μm wide, spaced by 150, 50, and 25 μm, respectively, on capillaries threaded with fine ferromagnetic wire.

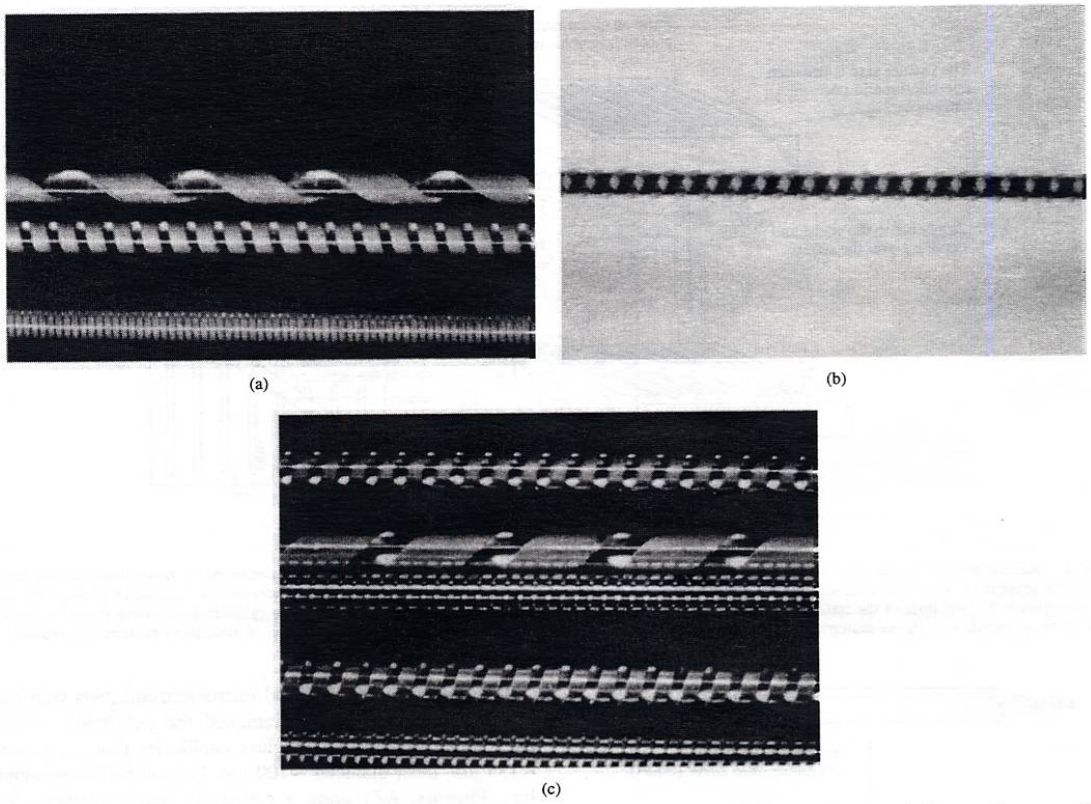

Fig. 4. Microcoils formed using microcontact printing. (a) Copper (thickness ~1 μm) coils consisting of wires 150, 50, and 25 μm wide separated by 150, 50, and 25 μm, respectively, on optical fibers (diameter = 125 μm). These coils resulted from printing palladium colloids followed by electroless deposition of copper. (b) Silver (thickness ~400 Å) double-helical coil made from wire 50 μm wide separated by 50 μm on a glass capillary (outer diameter = 135 μm). These coils were produced by using a resist of hexadecanethiol printed onto a capillary coated with silver. (c) Silver, gold, and copper (thickness ~3 μm) coils with wires 150, 50, and 25 μm wide separated by 150, 50, and 25 μm on glass capillaries (outer diameter = 135 μm). These coils were formed by electroplating silver, gold, and copper on coils of silver. From top to bottom, the coils are made of copper, gold, silver, gold, and silver. Original photograph in color. (Photographs in (a) and (c) by Felice Frankel.)

Also, using two electrically independent coils wrapped around adjacent regions of a single capillary threaded with ferromagnetic wire, we measured the voltage induced in one of the coils (the detecting coil) by passing current through the other (the exciting coil).

III. Results and Discussion

In this Section, we present several examples of conducting microcoils formed using the methods described above. We also summarize the electrical measurements performed on these structures and interpret the results.

A. Conducting Microcoils Formed Using Microcontact Printing

We used the method described in the experimental procedures to form conducting microcoils from wires with widths and spacings between 150–25 μm on cylinders with diameters between 100–400 μm (Fig. 4). Fig. 4(a) shows microcoils of copper fabricated by printing palladium colloids onto optical fibers and depositing copper onto these samples using an electroless plating bath [33]. Although it is possible to form microcoils using this procedure, we found that printing resists of hexadecanethiolate monolayers on silver substrates produced a higher yield of coils. Fig. 4(b) shows a double-helical coil of silver on a glass capillary stripped of its polymeric coating that was produced using this method. In this case, coils as long as a few centimeters that were free of opens or shorts could be fabricated with ~80% yield. Most failures were due to imperfections in the evaporated silver.

Coils like the one shown in Fig. 4 can be thickened by electrodeposition. Fig. 4(c) shows single-helical microcoils of copper, silver, and gold (thicknesses ~1–5 μm) formed by electroplating copper, silver, and gold. Thickening the coils in this manner decreases their electrical resistance and increases their mechanical rigidity. Approximately 80% of the thin coils that we electroplated formed thick coils free of opens or shorts. Most failures during the plating step were caused by attachment and welding of particulate impurities in the plating bath to the wires of the coils. We note that free-

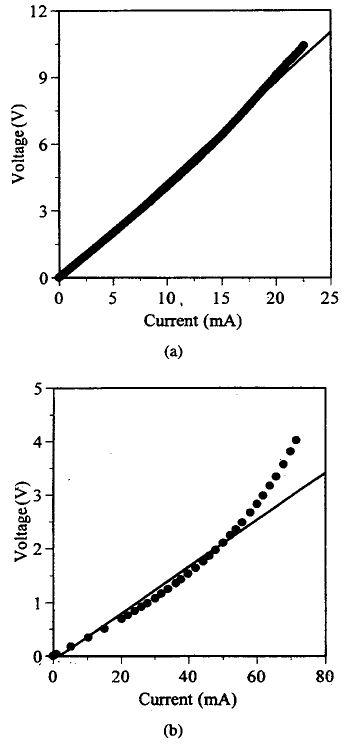

Fig. 5. Current measured as a function of voltage applied to silver (thickness ~400 Å, length = 1.0 cm) and gold (thickness ~2 μm, length = 0.65 cm) coils with 50-μm wire separated by 50 μm. In both cases, current was applied up to the point at which the coils ceased to conduct.

standing microcoils could be produced by dissolving the glass support with HF after electroplating. These free-standing coils were self-supporting and elastically deformable [35] and may have applications as mechanical components of more complex microelectromechanical systems (MEMS) devices.

B. Results and Interpretation of Electrical Measurements on Conducting Microcoils

1) Results and Qualitative Interpretation: Fig. 5 illustrates the current as a function of voltage applied to microcoils consisting of silver and gold wire 50 μm wide, separated by 50 μm and with thicknesses of ~300 Å (part A) and ~3 μm (part B). This figure shows that the resistance and the current at failure of the microcoil made with thick wire are lower and higher, respectively, than the microcoil made with thin wire. The curvature in the plot of voltage and current for the thick coil is likely the result of resistive heating that causes an increase in resistance. We believe that failure of the coils at high currents was caused by resistive heating that generated breaks in the wires.

Fig. 6 illustrates the inductance and resistance of a coil made from wire 25 μm wide separated by 25 μm and electroplated with gold to a thickness of a few microns, measured with a

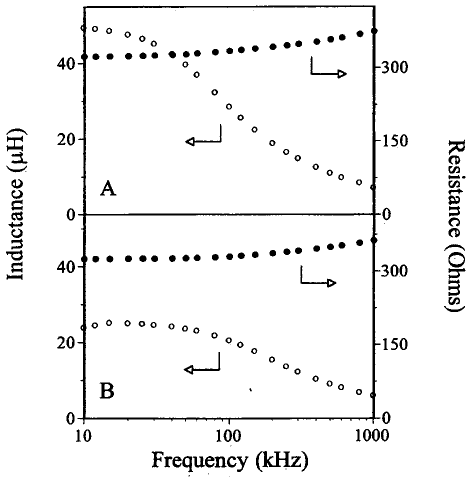

Fig. 6. Frequency dependence of the inductance and resistance of an inductor based on a coil of wire 25 μm wide and separated by 25 μm, printed on a capillary threaded with ferromagnetic wire. (a) shows the inductance and resistance when 0.1 mA is used for the testing current; (b) shows the inductance and resistance when 0.1 mA is used for the testing current, and a constant direct current of 5.0 mA is applied. The dependence of the inductance on frequency agrees with that observed previously in different systems [10]. The decrease in the inductance with increased bias current results from the nonlinearity of the permeability of the core.

test current of 0.1 mA and bias currents of 0.0 mA (a) and 5.0 mA (b). The decrease in inductance with increasing frequency is due to a dependence of the permeability of the core on the frequency that is at least partly associated with eddy–current losses. The decrease in inductance with increasing bias is due to the dependence of the permeability of the core on the magnitude of the current. It is likely that this dependence is due to saturation of the core. Similar behavior was observed recently in a similar system [10].

The inductances of coils with various lengths (0.6, 0.8, and 1.3 cm) and with wires of different widths and spaces (150, 50, and 25 μm) were also determined. Fig. 7(a) shows inductances of inductors with coils of different lengths at three frequencies. This figure shows that for a given number of turns per-unit length, the inductance is a linear function of the length of the coil. Fig. 7(b) shows measurements of the inductance per-unit length of coils made from wires with different widths. This figure shows that the inductance per-unit length is a quadratic function of the number of turns per-unit length. (We note that the inductance changed by ~15% as different segments of ferromagnetic wire were introduced into the core. We believe that inhomogeneities in the wire caused this variation.)

Fig. 8 illustrates the inductance as a function of dc bias current at 100 kHz with a test current of 0.1 mA for a coil fabricated with gold-plated wire 50-μm wide separated by 50 μm. The decrease in inductance with increasing bias, which is also illustrated in Fig. 6, suggests a saturation of the permeability of the ferromagnetic core.

Finally, Fig. 9 shows the voltage applied to the exciting coil and the voltage induced in the detecting coil of the assembly

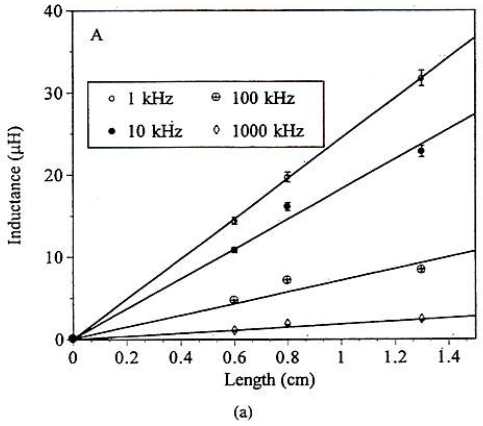

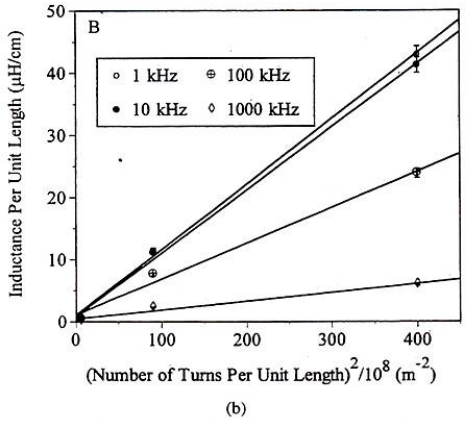

Fig. 7. (a) Inductance and resistance of three different lengths of inductors based on coils of wire 50 μm wide and separated by 50 μm, printed on a capillary threaded with ferromagnetic wire. Measurements were performed at 1, 10, 100, and 1000 kHz with a testing current of 0.1 mA. The inductances show a linear dependence on the length. (b) Inductance for electromagnets with three different turns per-unit length measured at 1, 10, 100, and 1000 kHz with a testing current of 0.1 mA. The inductances show a linear dependence on the square of the number of turns per-unit length. These results are consistent with the behavior of a simple ideal solenoidal inductor.

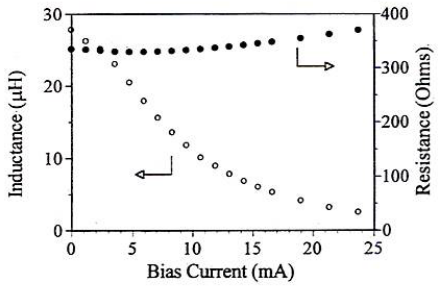

Fig. 8. Inductance for an inductor based on a coil of wire 50 μm wide and separated by 50 μm, printed on a capillary threaded with ferromagnetic wire. The inductance was measured at 100 kHz with a testing current of 0.1 mA at different values of direct current bias. The data show a decrease in the inductance with increasing bias. This behavior is consistent with a saturation of the core.

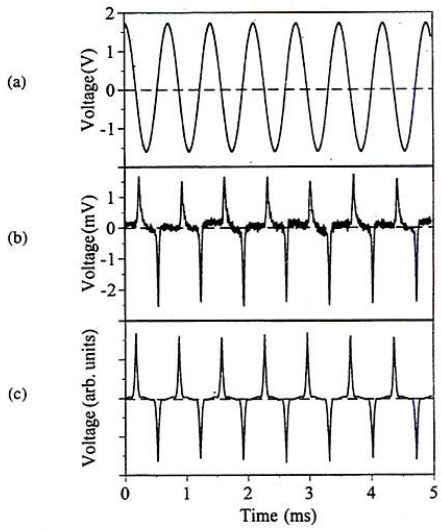

Fig. 9. A sinusoidally varying voltage applied to an exciting coil gives rise to a changing magnetic flux that induces a voltage in a detecting coil. (a) Voltage applied to the exciting coil. (b) Voltage induced in a detecting coil by the adjacent exciting coil. The nonlinear behavior of the induced voltage is consistent with a saturation of the magnetization of the core. (c) Simulation of voltage induced in a detecting coil by the adjacent exciting coil. The behavior of the simulated voltage was determined by the dependence of the inductance on the current, as illustrated in Fig. 6. These simulations are qualitatively consistent with measurements illustrated in (a) and are consistent with saturation of the core.

described previously. These data indicate that the changing magnetic flux created by the exciting coil in the detecting coil is nonlinearly related to the voltage across the excitation coil. The form of this strongly nonlinear relationship is consistent with magnetic saturation in the core.

2) Quantitative Interpretation: We computed the magnetic field of a solenoid with dimensions similar to those of the fabricated structures. The computations show that the magnetic field is uniform and much like an ideal solenoid in the central region of the spiral (Fig. 10). Since the ferromagnetic cores of our inductors occupy only this central location, the computations suggest that our electromagnets and inductors can be treated, to a good approximation, as ideal solenoids.

For an ideal solenoid, the inductance L is related to the geometry of the structure and to the permeability of the material making up the core according to

$$L = \mu_r \mu_o N^2 \pi r^2 \ell = B \pi r^2 N \ell / i. \tag{2}$$

In this expression, μ_o is the permeability of free space, μ_r is the effective relative permeability of the core, N is the turns per-unit length, ℓ is the length, r is the radius of the cylindrical support, B is the magnitude of the magnetic field, and i is the current. The linear dependence of the inductance on the length shown in Fig. 7(a) and the quadratic dependence of the inductance per-unit length on the number

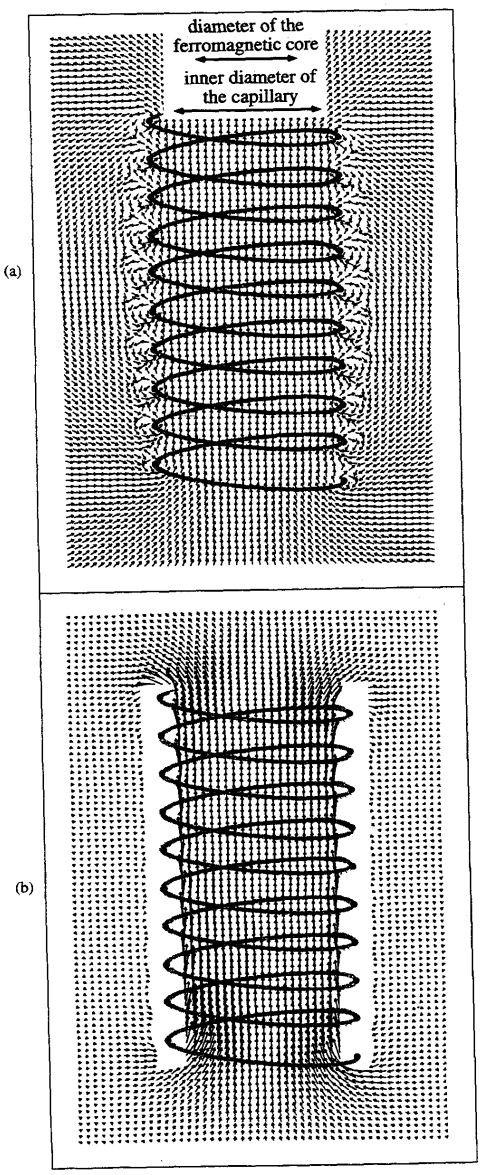

Fig. 10. Computations of (a) the magnetic-field direction and (b) the magnetic field for a loosely wound solenoid. The results indicate that even with a loosely wound geometry, at the position of the ferromagnetic core in the microinductors described in this paper, the magnetic field is highly uniform and points purely along the axis of the capillary. These results indicate that the microelectromagnets studied here can be treated to a first approximation as ideal solenoids.

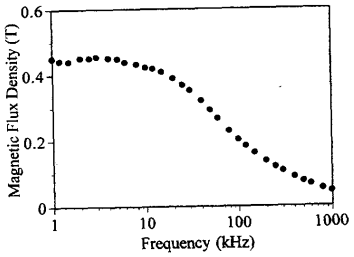

Fig. 11. Magnetic flux density as a function of frequency computed from inductances measured in an inductor with a testing current of 10.0 mA. The inductor was 1.2 cm long and used a coil with wire that was 25 μm wide and separated by 25 μm.

of turns per-unit length shown in Fig. 7(b) are consistent with both (2) and the results of calculations shown in Fig. 10 that indicate a uniform field in the central region of the solenoid.

Using (2) and the geometry of one of our electromagnets (i.e., $\ell = 1.2$ cm, $N = 2.0 \times 10^4$ turns/meter, and $r = 40$ μm), we computed the magnetic field in the core of the electromagnet (Fig. 11) from the data similar to that shown in Fig. 6, but collected with a testing current of 10.0 mA. Based on data illustrated in Figs. 6 and 8, we believe that the maximum magnetic flux density ($\sim$0.4 T) is limited only by magnetic saturation of the core. (We note that the flux density computed in this way represents an approximate value. It ignores limitations associated with using an LCR meter to determine the inductance of a nonlinear inductor.)

Measurements illustrated in Fig. 9(b) provide additional evidence that saturation of the magnetization of the core limits the magnetic flux density. Using the measured dependence of the inductance on the current and the fact that the inductors are primarily resistive, we calculated the temporal behavior of the voltage induced in the detecting coil by passing sinusoidal current through the exciting coil. The results, shown in Fig. 9(c), are consistent with the measured results shown in Fig. 9(b). The asymmetry in the voltage spikes measured in detecting coil and the offset of these spikes from the zero crossing of the voltage in the exciting coil [neither of which are reproduced in the simple modeling results shown in Fig. 9(c)] are possibly due to small dc currents induced in the exciting coil by the function generator driving this coil, small magnetic fields present in the lab, or to hysteresis in the core.

IV. Conclusion

We have demonstrated that μCP can be used to form single- and multiple-helical microcoils by printing lines on cylindrical objects. Although coils shown here were made with wire with widths and separations greater than 25 μm, μCP works well into the submicron range. Because our printing apparatus provides the ability to set the orientation of the stamp and the cylinders to better than 0.1°, for cylinders with diameters less than $\sim$125 μm, we do not anticipate any

fundamental or practical difficulties associated with reducing the widths of the wires of the smallest coils by an order of magnitude. In addition, we believe that the printing process can be automated with the addition of motorized stages and that it will be possible to print many capillaries simultaneously.

We also described the performance of our microfabricated coils as elements in microelectromagnets and microinductors. Electrical measurements indicated inductances in the range of microhenry and flux densities as large as ~0.4 T. The data suggest that the saturation point of our core material limits the maximum magnetic flux density. It should be possible, therefore, to increase the magnetic flux density of the electromagnets by using a ferromagnetic core with a higher saturation point. For example, with or without electroplating, our coils can provide the required number of ampere-turns per-unit length (~200 A · turn/meter) to access the entire hysteresis loop for iron, a material that begins to saturate near 1 T [36].

Finally, although we focused on the use of microcoils for microinductors and microelectromagnets, there are many non-electrical uses for microcoils. Examples include microsprings, screws, and other components with possible applications in MEMS and coils for various surgical uses [37].

ACKNOWLEDGMENT

The authors thank F. Frankel for photography [Fig. 4(a) and 4(c)].

REFERENCES

[1] D. L. Olson, T. L. Peck, A. G. Webb, R. L. Magin, and J. V. Sweedler, "High-resolution microcoil H-NMR for mass-limited, nanoliter-volume samples," *Science*, vol. 270, no. 5244, pp. 1967–1970, 1995.

[2] T. L. Peck, R. L. Magin, and P. C. Lauterbur, "Design and analysis of microcoils for NMR microscopy," *J. Magn. Resonance, Series B*, vol. 108, no. 2, pp. 114–124, 1995.

[3] T. L. Peck, R. L. Magin, J. Kruse, and M. Feng, "NMR microspectroscopy using 100 mm planar RF coils fabricated on gallium arsenide substrates," *IEEE Trans. Biomed. Eng.*, vol. 41, no. 7, pp. 706–709, 1994.

[4] J. S. Schoeniger and S. J. Blackband, "The design and construction of a NMR microscopy probe," *J. Magn. Resonance Series B*, vol. 104, no. 2, pp. 127–134, 1994.

[5] *Recent Magnetics for Electronics, Japan Annual Reviews in Electronics, Computers and Telecommunications*, OHM, North Holland, NY, vol. 15, 1984.

[6] *IEEE Trans. Magn.*, vol. 31, no. 6, 1995.

[7] F. Primdahl, "The fluxgate magnetometer," *J. Phys. E: Sci. Instrum.*, vol. 12, pp. 241–253, 1979.

[8] T. Seitz, "Fluxgate sensor in planar technology," *Sens. Actuators*, vols. A21–A23, pp. 799–802, 1990.

[9] P. Ripka, "Review of fluxgate sensors," *Sens. Actuators A*, vol. 33, no. 3, pp. 129–141, 1992.

[10] S. Kawahito, Y. Sasaki, H. Sato, T. Nakamura, and Y. Tadokoro, "A fluxgate magnetic sensor with micro-solenoids and electroplated permalloy cores," *Sens. Actuators A*, vol. 43, no. 1, pp. 128–134, 1994.

[11] J. A. Nyenhuis, J. C. Treece, J. M. Drynan, H. A. Sabbagh, and L. D. Sabbagh, "Data scquisition for experimental verification of an eddy current model for three dimensional inversion," *IEEE Trans. Magn.*, vol. 23, no. 3, pp. 3789–3791, 1987.

[12] M. Uesaka, T. Nakanishi, K. Miya, H. Komatsu, K. Aoki, and K. Kasai, "Micro eddy current testing by micro magnetic sensor array," *IEEE Trans. Magn.*, vol. 31, no. 1, pp. 870–876, 1995.

[13] T. Hirota, T. Siraiwa, K. Hiramoto, and M. Ishihara, "Development of micro-coil sensor for measuring magnetic field leakage," *Japanese J. Appl. Phys.*, vol. 32, no. 7, pp. 3328–3329, 1993.

[14] W. Wang and T. He, "A high precision micropositioner with five degree of freedom based on an electromagnetic driving principle," *Rev. Sci. Instrum.*, vol. 67, no. 1, pp. 312–317, 1996.

[15] B. Wagner, W. Benecke, G. Engelmann, and J. Simon, "Microactuators with moving magnets for linear, torsional or multiaxial motion," *Sens. Actuators A*, vol. 32, nos. 1–3, pp. 598–603, 1992.

[16] I. J. Busch-Vishniac, "The case of magnetically driven microactuators," *Sens. Actuators A*, vol. 33, no. 3, pp. 207–220, 1992.

[17] F. Amblard, B. Yurke, A. Pargellis, and S. Leibler, "A magnetic manipulator for studying local rheology and micromechanical properties of biological systems," *Rev. Sci. Instrum.*, vol. 67, no. 3, pp. 818–827, 1996.

[18] M. Yamaguchi, S. Arakawa, H. Ohzeki, Y. Hayashi, and K. I. Arai, "Characteristics and analysis of a thin film inductor with closed magnetic circuit structure," *IEEE Trans. Magn.*, vol. 28, no. 5, pp. 3015–3017, 1992.

[19] M. Yamaguchi, S. Arakawa, S. Yabukami, K. I. Arai, F. Kumagai, and S. Kikuchi, "Estimation of the in-situ permeabilities in thin-film inductors," *IEEE Trans. Magn.*, vol. 29, no. 6, pp. 3210–3212, 1993.

[20] Y. Kobayashi, S. Ishibashi, K. Shirakawa, J. Toriu, H. Matsuki, and K. Murakami, "New type micro cloth-inductor and transformer with thin amorphous wires and multi-thin coils," *IEEE Trans. Magn.*, vol. 28, no. 5, pp. 3012–3014, 1992.

[21] O. Oshiro, H. Tsujimoto, and K. Shirae, "A novel miniature planar inductor," *IEEE Trans. Magn.*, vol. 23, no. 5, pp. 3759–3761, 1987.

[22] K. Yamaguchi, S. Ohnuma, T. Imagawa, J. Toriu, H. Matsuki, and K. Murakami, "Characteristics of a thin film microtransformer with circular spiral coils," *IEEE Trans. Magn.*, vol. 29, no. 5, pp. 2232–2237, 1993.

[23] K. Yamaguchi, E. Sugawara, O. Nakajuma, H. Matsuki, and K. Murakami, "Load characteristics of a spiral coil type thin film microtransformer," *IEEE Trans. Magn.*, vol. 29, no. 6, pp. 3207–3209.

[24] K. Kurata, K. Shirakawa, O. Nakazima, and K. Murakami, "Study of thin film micro transformer with high operating frequency and coupling coefficient," *IEEE Trans. Magn.*, vol. 29, no. 6, pp. 3204–3206, 1993.

[25] M. Mino, T. Yachi, A. Tago, K. Yanagisawa, and K. Sakakibara, "A new planar microtransformer for use in micro-switching converters," *IEEE Trans. Magn.*, vol. 28, no. 4, pp. 1969–1973, 1992.

[26] J. V. Sweedler, personal communication.

[27] P. F. Nealey, A. J. Black, J. L. Wilbur, and G. M. Whitesides, "Micro- and nanofabrication techniques based on self-assembled monolayers," *Molecular Electronics*, J. Jortner and M. Ratner, Eds. Oxford, U.K.: Blackwell Science, 1997.

[28] A. Kumar and G. M. Whitesides, "Features of gold having micrometer to centimeter dimensions can be formed through a combination of stamping with an elastomeric stamp and an alkanethiol ink," *Appl. Phys. Lett.*, vol. 63, no. 14, p. 2002, 1993.

[29] A. Kumar, H. A. Biebuyck, N. L. Abbott, and G. M. Whitesides, "The use of self-assembled monolayers and a selective etch to generate patterned gold features," *J. Amer. Chem. Soc.*, vol. 114, p. 9188, 1992.

[30] R. J. Jackman, J. L. Wilbur, and G. M. Whitesides, "Fabrication of submicron features on curved substrates by microcontact printing," *Science*, vol. 269, no. 5224, p. 664, 1995.

[31] Y. Xia, E. Kim, and G. M. Whitesides, "Microcontact printing of alkanethiols on silver and its application in microfabrication," *J. Electrochem. Soc.*, vol. 143, no. 3, pp. 1070–1079, 1996.

[32] P. M. St. John and H. G. Craighead, "Microcontact printing and pattern trasfer using trichlorosilanes on oxide substrates," *Appl. Phys. Lett.*, vol. 68, no. 7, pp. 1022–1024, 1996.

[33] P. C. Hidber, W. Helbig, E. Kim, and G. M. Whitesides, "Microcontact printing of palladium colloids—Micron-scale patterning by electroless deposition of copper," *Langmuir*, vol. 12, no. 5, p. 1375, 1996.

[34] J. A. Rogers, R. J. Jackman, G. M. Whitesides, J. L. Wagener, and A. M. Vengsarkar, "Using microcontact printing to generate amplitude photomasks on the surfaces of optical fibers: A new method for producing in-fiber gratings," *Appl. Phys. Lett.*, vol. 70, no. 1, p. 7, 1997.

[35] J. A. Rogers, R. J. Jackman, and G. M. Whitesides, "Microcontact printing and electroplating on curved substrates: A means for producing free-standing three-dimensional metallic microstructures with possible applications ranging from micro-coil springs to coronary stents," *Adv. Mater.*, vol. 9, no. 6, pp. 475–477, 1997.

[36] P. Lorrain and D. Corson, *Electromagnetic Fields and Waves*, 2nd ed. San Fransisco, CA: Freeman, p. 398, 1970.

[37] L. H. Monsein, "New detachable coils for treating cerebral aneurysms," *Nature Medicine*, vol. 2, no. 2, pp. 160–161, 1996.

John A. Rogers was born in 1967 in Rolla, MO. He received the B.A. and B.S. degrees in chemistry and physics from the University of Texas, Austin, in 1989 and the S.M. degrees in physics and chemistry in 1992 and the Ph.D. degree in physical chemistry in 1995 from MIT, Cambridge, MA.

From 1995 to 1997, he was a Junior Fellow in the Harvard University Society of Fellows. He is now a Member of the Technical Staff in Condensed Matter Physics at Bell Laboratories, Lucent Technologies, Murray Hill, NJ. His current interests include micro and nanofabrication, MEMS, MOMS, optics, and the use of ultrafast lasers for coherent time-resolved spectroscopy.

Rebecca J. Jackman was born in Farnham, Surrey, U.K., in 1971. She received the B.Sc. degree in chemistry from McGill University, Montreal, Canada, in 1993. She is currently working toward the Ph.D. degree in chemistry at Harvard University, Cambridge, MA.

Her research interests include the use of self-assembly in the fabrication of 3-D micro and nanostructures for use in microelectromechanical, microoptomechanical, and microfluidic systems.

George M. Whitesides was born on August 3, 1939 in Louisville, KY. He received the A.B. degree from Harvard University, Cambridge, MA, in 1960 and the Ph.D. degree from the California Institute of Technology, Pasadena, in 1964.

He was a Member of the Faculty of the Massachusetts Institute of Technology, Cambridge, MA, from 1963 to 1982. He joined the Department of Chemistry, Harvard University, in 1982 and was Department Chairman from 1986 to 1989. He is now Mallinckrodt Professor of Chemistry at Harvard University. His present research interests include biochemistry, surface chemistry, materials science, molecular virology, optics, self-assembly, and organic synthesis.